tektonika

Supporting Information (SI)

for

Unraveling the Kinematics and Morphotectonics of the Petrinja Fault (Croatia), Source of the 2020 M 6.4 Earthquake

Maxime Henriquet[1,2], Lucilla Benedetti[1], Stéphane Baize[3], Branko Kordić[4], Marianne Métois[5], Josipa Maslač Soldo[4], Nikola Belić[4], Marko Špelić[4], Marko Budić[4], Daniela Pantosti[6], Francesca Cinti[6], Stefano Pucci[6], Alessio Testa[7], Paolo Boncio[7], Bruno Pace[7], Petra Jamšek Rupnik[8], Adrien Moulin[9], Riccardo Civico[6]

[1]Aix Marseille Université, CNRS, IRD, Collège de France, CEREGE, Aix-en-Provence, France

[2]Université Côte d'Azur, CNRS, Observatoire de la Côte d'Azur, IRD, Géoazur, Valbonne, France

[3]Autorité de Sûreté Nucléaire et de Radioprotection, PSE-ENV/SCAN/BERSSIN, Fontenay-aux-Roses, France

[4]Croatian Geological Survey (HGI-CGS), Zagreb, Croatia

[5]Université Claude Bernard Lyon 1, Laboratoire de Géologie de Lyon, France

[6]Istituto Nazionale di Geofisica e Vulcanologia, Roma, Italy

[7]Università G. d'Annunzio Chieti – Pescara, Italy

[8]Geological Survey of Slovenia, Ljubljana, Slovenia

[9]Université Paris Cité, Institut de Physique Du Globe de Paris, CNRS, UMR 7154, Paris, France

Contents

Introduction

In the following we provide additional figures to show the topographic data free used to estimate fault offset with and without interpretations (Figures S1 to S5). We also summarize in the Figure S6 a compilation of offsets and potential ages of the geomorphological markers used in this study to determine fault slip rates. Finally, the Table S1 shows the full chemical composition (major and traces elements) analyzed at the Service d'Analyse des Roches et des Minéraux (SARM) for six carbonate samples used to determine the ^{36}Cl concentration (see the corresponding Table 1).

 https://doi.org/10.55575/tektonika2026.4.1.104

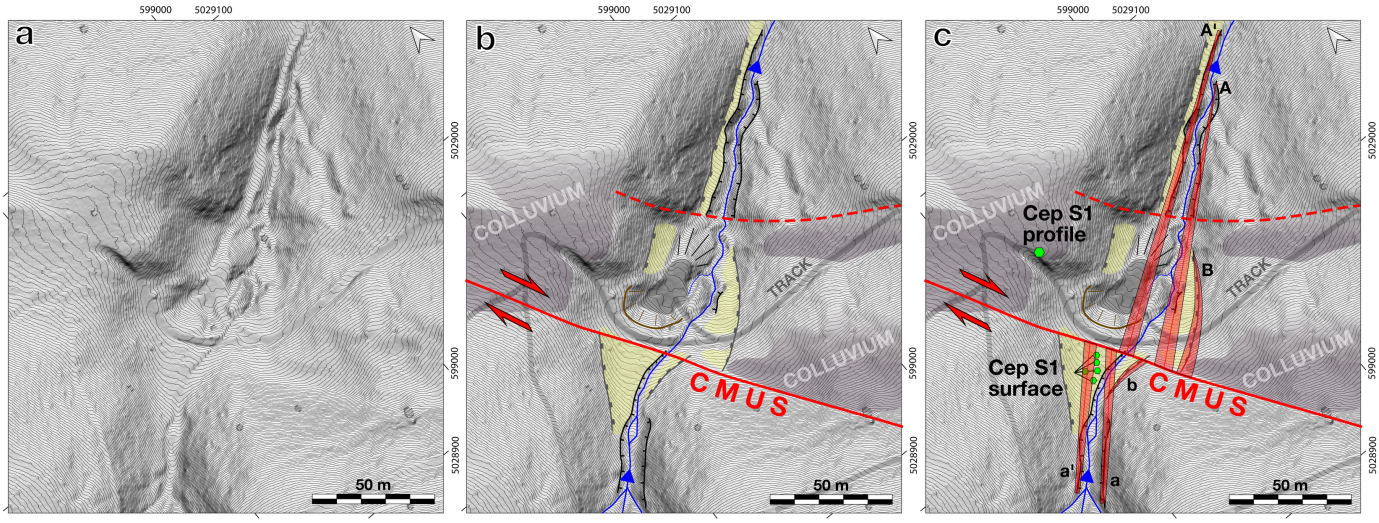

Figure S1: Geomorphological mapping and piercing lines used to estimate fault offsets at the Cepeliš site S1 on the CMUS. Panel a) High-resolution shaded LiDAR DEM (50 cm contour line spacing). Panel b) Geomorphological interpretation. Panel c) Geomorphological interpretation and location of 3 sets of piercing lines corresponding to inner and outer terrace risers. Estimated offsets are given in the associated Figure 6b.

 https://doi.org/10.55575/tektonika2026.4.1.104

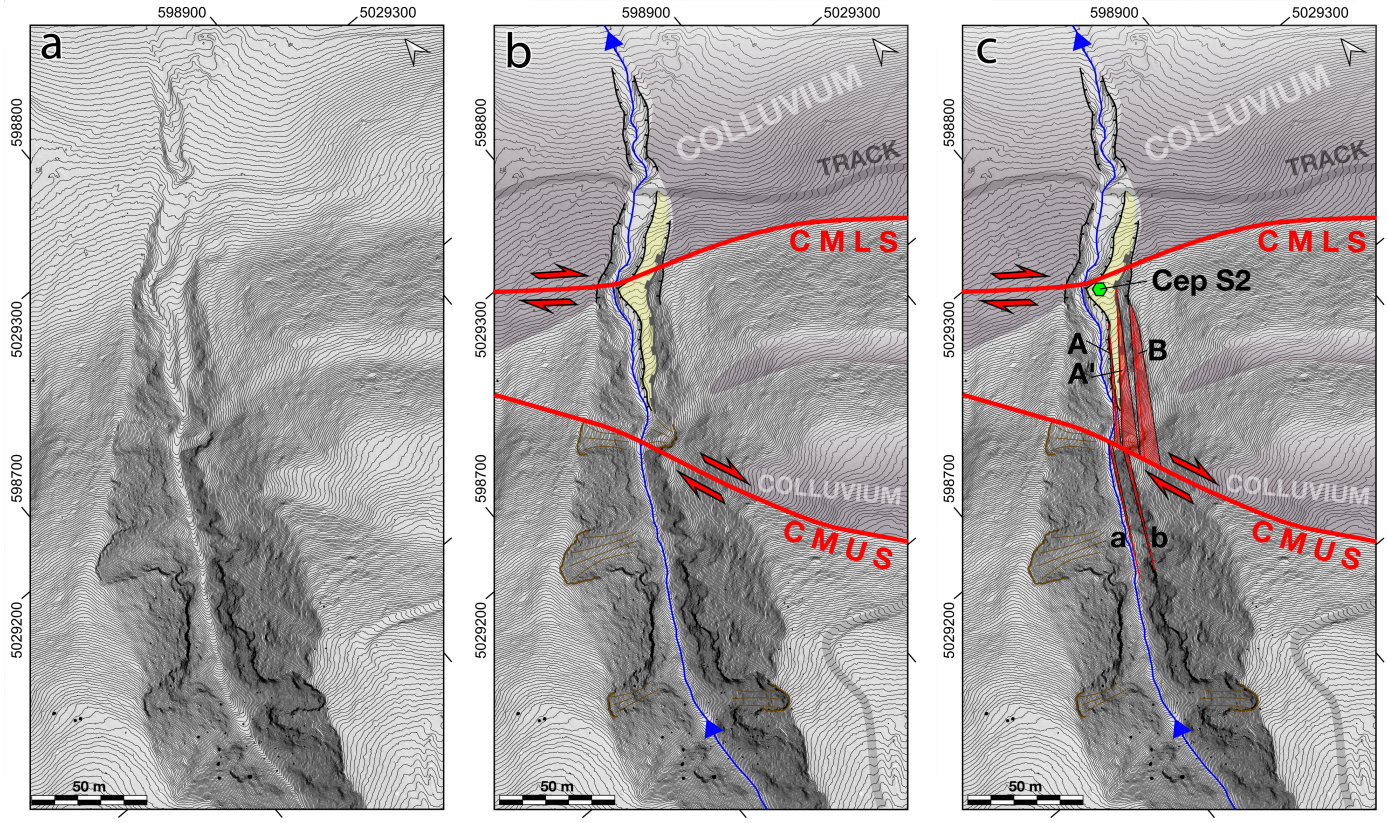

Figure S2: Geomorphological mapping and piercing lines used to estimate fault offsets at the Cepeliš site S2a on the CMUS. Panel a) High-resolution shaded LiDAR DEM (50 cm contour line spacing). Panel b) Geomorphological interpretation. Panel c) Geomorphological interpretation and location of 3 sets of piercing lines corresponding to inner and outer terrace risers as well as river incision scarps. Estimated offsets are given in the associated Figure 8b.

https://doi.org/10.55575/tektonika2026.4.1.104

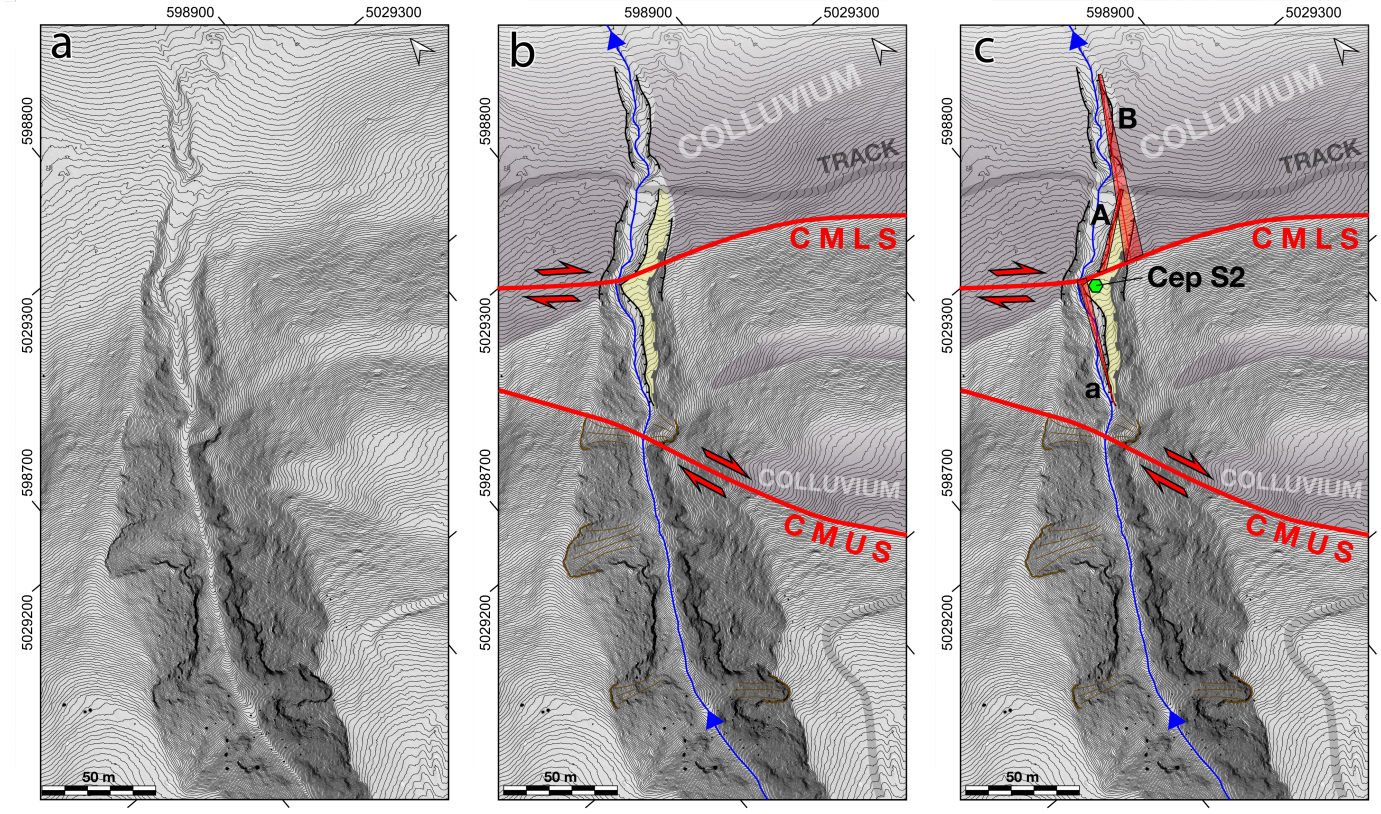

Figure S3: Geomorphological mapping and piercing lines used to estimate fault offsets at the Cepeliš site S2b on the CMLS. Panel a) High-resolution shaded LiDAR DEM (50 cm contour line spacing). Panel b) Geomorphological interpretation. Panel c) Geomorphological interpretation and location of 2 sets of piercing lines corresponding to the outer terrace risers. Estimated offsets are given in the associated Figure 9b.

https://doi.org/10.55575/tektonika2026.4.1.104

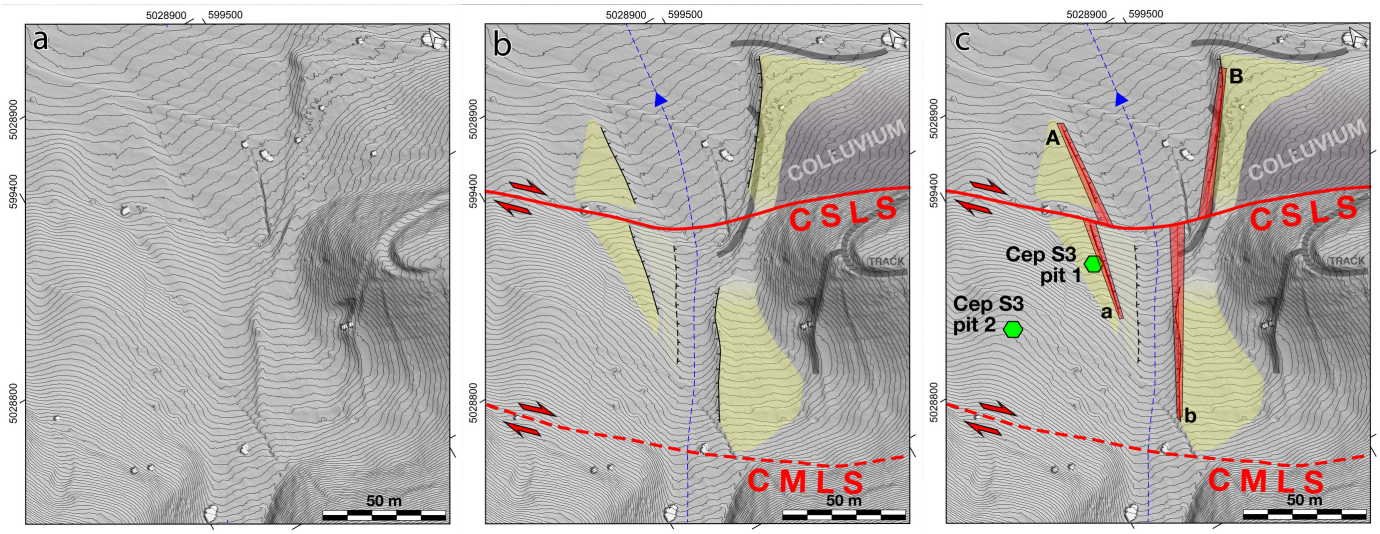

Figure S4: Geomorphological mapping and piercing lines used to estimate fault offsets at the Cepeliš site S3 on the CSLS. Panel a) High-resolution shaded LiDAR DEM (50 cm contour line spacing). Panel b) Geomorphological interpretation. Panel c) Geomorphological interpretation and location of 2 sets of piercing lines corresponding to the outer terrace risers. Estimated offsets are given in the associated Figure 11b.

https://doi.org/10.55575/tektonika2026.4.1.104

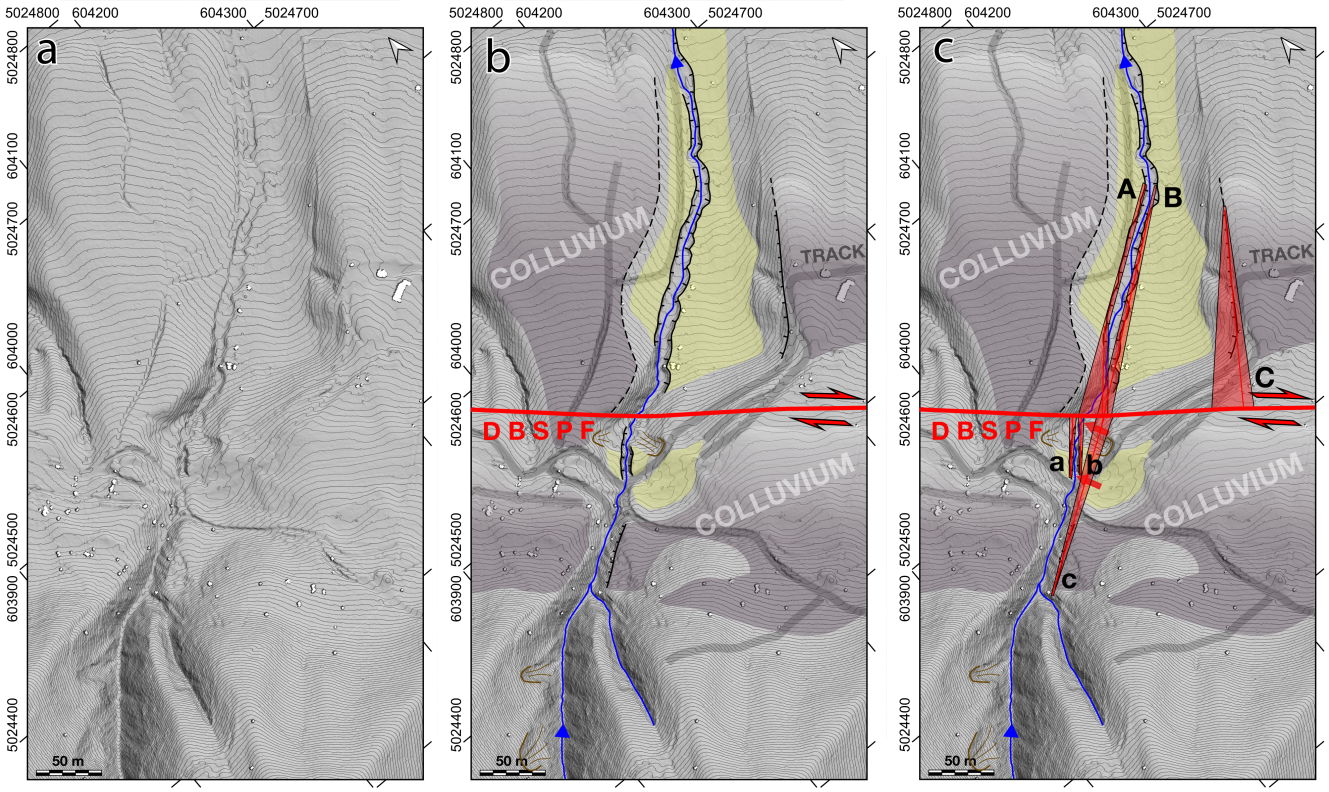

Figure S5: Geomorphological mapping and piercing lines used to estimate fault offsets at the Gornja Budičina on the DBSPF. Panel a) High-resolution shaded LiDAR DEM (50 cm contour line spacing). Panel b) Geomorphological interpretation. Panel c) Geomorphological interpretation and location of 3 sets of piercing lines corresponding to the inner and outer terrace risers. Estimated offsets are given in the associated Figure 14b.

https://doi.org/10.55575/tektonika2026.4.1.104

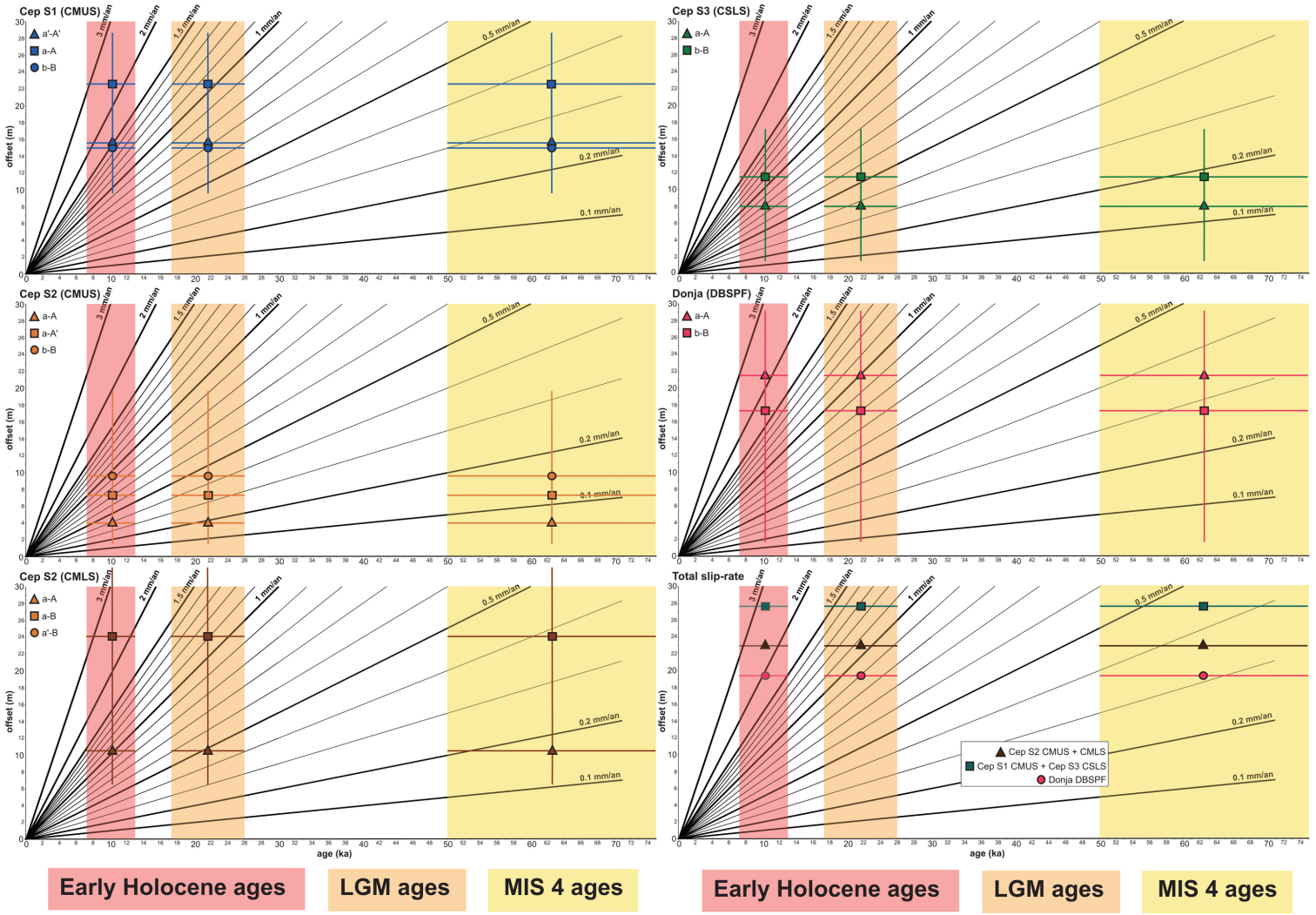

Figure S6: Offsets and potential ages of the geomorphological markers. 4 sites were studied at Cepeliš (Cep S1, S2a, S2b and S3) on the CMUS, CMLS and CSLS fault strands, and one to the SE on the DBSPF fault strand from the Gornja Budičina site (panels a to e). The last plot (panel f) shows a combination of the offsets from the Cepeliš S2a and S2b sites (CMUS + CMLS), the Cepeliš S1 and S3 sites (CMUS + CSLS), and the offsets from the Donja Budicina site on the DBSPF. The blue and yellow transparent bars represent the range of potential ages of offset formation considering the MIS 4 (50-75 ka), LGM (17.3-26 ka) or Early Holocene (7.2-13 ka) hypotheses. The diagonal lines indicate the slip rates.

 https://doi.org/10.55575/tektonika2026.4.1.104

Sample	As µg/g	Ba µg/g	Be µg/g	Bi µg/g	Cd µg/g	Co µg/g	Cr µg/g	Cs µg/g	Cu µg/g	Ga µg/g	Ge µg/g	Hf µg/g	In µg/g	Mo µg/g	Nb µg/g	Ni µg/g	Pb µg/g	Rb µg/g	Sb µg/g	Sc µg/g	Sn µg/g	Sr µg/g
Cep_S1_1	3,68	72,9	0,32	< L.D.	0,26	1,18	21,2	0,92	3,2	2,50	0,35	1,82	< L.D.	< L.D.	2,48	6,5	2,51	19,5	0,73	1,83	0,54	617
Cep_S1_2	2,25	56,5	0,25	< L.D.	0,24	0,79	20,3	0,59	2,1	1,80	0,28	1,29	< L.D.	< L.D.	1,86	4,2	2,07	14,1	0,45	1,37	0,35	508
Cep_S1_12	6,31	68,7	0,55	0,08	0,24	3,86	30,5	2,63	11,3	4,66	0,35	1,34	< L.D.	0,79	3,41	23,5	5,37	25,9	1,08	3,97	1,07	494
Cep_S1_6	3,13	34,3	0,30	< L.D.	0,37	2,72	18,5	1,11	6,6	2,07	0,16	0,58	< L.D.	< L.D.	1,44	10,9	2,64	11,4	0,54	1,89	0,54	599
Cep_S3_2	1,88	87,8	0,36	< L.D.	0,12	0,71	26,1	0,68	2,3	2,32	0,39	1,08	< L.D.	< L.D.	1,90	4,1	2,14	19,3	0,55	1,70	0,53	498
Cep_S3_3	5,31	85,0	0,52	< L.D.	0,26	1,73	40,7	0,95	4,2	3,01	0,57	1,75	< L.D.	< L.D.	2,54	10,1	3,17	18,9	0,93	2,68	0,51	488

	Ta µg/g	Th µg/g	U µg/g	V µg/g	W µg/g	Y µg/g	Zn µg/g	Zr µg/g	La µg/g	Ce µg/g	Pr µg/g	Nd µg/g	Sm µg/g	Eu µg/g	Gd µg/g	Tb µg/g	Dy µg/g	Ho µg/g	Er µg/g	Tm µg/g	Yb µg/g	Lu µg/g
Cep_S1_1	0,25	2,11	3,56	17,5	< L.D.	6,32	9,9	70,4	6,77	13,3	1,68	6,58	1,39	0,259	1,17	0,178	1,07	0,227	0,601	####	0,605	0,094
Cep_S1_2	0,20	1,39	2,42	12,3	< L.D.	5,15	7,2	48,1	5,27	10,6	1,30	5,15	1,07	0,204	0,911	0,141	0,876	0,180	0,489	####	0,471	0,076
Cep_S1_12	0,33	2,70	5,48	39,2	< L.D.	9,09	21,2	50,4	8,51	16,5	2,03	7,82	1,64	0,322	1,43	0,230	1,42	0,302	0,815	0,124	0,801	0,124
Cep_S1_6	0,13	1,17	5,26	25,1	< L.D.	4,74	10,8	21,4	4,17	7,14	0,954	3,71	0,786	0,163	0,700	0,109	0,669	0,145	0,394	####	0,378	0,059
Cep_S3_2	0,20	1,65	1,81	15,4	< L.D.	7,83	7,8	42,5	8,20	10,8	1,88	7,39	1,55	0,325	1,40	0,219	1,30	0,265	0,708	0,103	0,660	0,096
Cep_S3_3	0,23	2,15	3,39	18,8	< L.D.	11,1	15,9	70,0	12,8	14,8	2,90	11,6	2,37	0,481	2,05	0,306	1,80	0,366	0,937	0,140	0,875	0,132

	SiO2 %	Al2O3 %	Fe2O3 %	MnO %	MgO %	CaO %	Na2O %	K2O %	TiO2 %	P2O5 %	PF %	Total %
Cep_S1_1	19,40	2,14	0,50	< L.D.	0,53	41,78	0,23	0,65	0,13	< L.D.	34,20	99,55
Cep_S1_2	15,89	1,62	0,33	< L.D.	0,41	44,94	0,21	0,48	0,099	< L.D.	35,91	99,89
Cep_S1_12	11,55	3,50	1,40	< L.D.	0,88	44,31	0,07	0,63	0,20	< L.D.	37,31	99,84
Cep_S1_6	4,64	1,55	0,65	< L.D.	0,80	50,50	0,03	0,25	0,087	< L.D.	41,10	99,61
Cep_S3_2	19,53	2,20	0,66	< L.D.	0,55	41,91	0,41	0,72	0,099	< L.D.	34,07	#####
Cep_S3_3	19,78	2,69	1,35	0,027	0,61	40,61	0,54	0,64	0,16	< L.D.	33,15	99,55

Table S1: Full chemical composition (major and traces elements) of six samples (fraction < 250 µm) analyzed at the Service d'Analyse des Roches et des Minéraux (SARM).